

# Continuous Shape-Grinding Experiment Based on Constraint-Combined Force/Position Hybrid Control Method

Mamoru MINAMI\*, Hiro TANIMOTO\*, Akira YANOU\*, and Masaki TAKEBAYASHI\*

**Abstract:** Based on the analysis of the interaction between a manipulator's hand and a working object, a model representing the constrained dynamics of the robot is first discussed. The constraint forces are expressed by an algebraic function of states, input generalized forces, and constraint condition, and then direct position/force controller without force sensor is proposed based on the algebraic relation. To give the grinding system the ability to adapt to any object shape being changed by the grinding, we added estimating function of the constraint condition in real time for the adaptive position/force control, which is indispensable for our method instead of not using force sensor. Evaluations through continuous shape-grinding experiment by fitting the changing constraint surface with spline functions, indicates that reliable position/force control and shape-grinding work can be achieved by this proposed controller.

**Key Words:** shape-grinding, force/position control, on-line estimation of constraint surface.

## 1. Introduction

Many researches have discussed on the force control of robots for contacting tasks. Most force control strategies are to use force sensors [1]–[3] to obtain force information, where the reliability and accuracy are limited since the work-sites of the robot are filled with noise and thermal disturbances, reducing the sensor's reliability. On top of this, force sensors could lead to the falling of the structure stiffness of manipulators, which is one of the most essential defects for manipulators executing grinding tasks. To solve these problems, some approaches using no force sensor have been presented [4],[5]. To ensure the stabilities of the constrained motion, those force and position control methods have utilized Lyapunov's stability analysis under the inverse dynamic compensation [6]–[8]. Their force control strategies have been explained intelligibly in books [9],[10] and recently interaction control for six-degree-of-freedom tasks has been compiled in a book [11].

Those former classical robot controlling approaches can be classified into two broad categories [8]: impedance control and hybrid (force/position) control. In impedance control, a prescribed dynamic relation is sought to be maintained between the robot end-effector's force exerting to an object constraining the end-effector and position displacement toward the direction vertical to the object's surface [12]. In hybrid control, the end-effector's force is explicitly controlled in selected directions and the end-effector's position is controlled in the remaining (complementary) directions [1].

In the classified categories, our force/position control approach named as Constraint-Combined Control, which will be detailedly introduced later, belongs to model based hybrid control of rigid robot in hard contact with rigid environment. The

work-piece being ground by our grinding robot in this paper is iron, of which the spring constant is so huge to the extent that we can ignore the deformation of the work-piece caused by the contacting force with robot's end-effector. Hence, the contact process of the grinder can be just thought as non-dynamical process but a kinematical one, in which there is no motion occurred in vertical direction. Therefore, in this research we don't use the time-differential motion equation to analyze contacting vertical process to the work-piece, and on the contrary, we consider an algebraic equation as the constraint condition to analyze this contact vertical force. The Constraint-Combined Force Controller based on this algebraic equation has the ability to achieve the force control without time delay. Moreover, force error will not be affected by the dynamical motion along to the surface in horizontal direction. In model based hybrid control field, some former researches have noticed this "just an immediate contact result but no motion occurred" problem and try to solve it by using force or torque sensors. But since force or torque sensors are so costly, we consider a new force/position control method without using any sensors. Therefore, with these differences from those former force control methods, we can announce that the Constraint-Combined force/position control method without using sensors introduced in this paper can be thought to be essentially different from methods proposed so far. For example, a robot machining system for grinding, polishing and milling was developed [13] recently, but the system uses just position control of robot tip through scanned surface profile without considering any force control. P. Hamelin et al.[14] have considered underwater direct-drive grinding robot in order to repair dikes and dams periodically for operability. This research focused on trajectory-tracking performance and it did not mention about force control even though a constant grinding force was assumed to be applied on workpiece. Y. Song et al.[15] proposed a robot belt grinding system that uses a force/position hybrid control method. Different from the authors' system, their method uses force sensors to control the contact force. Position

\* Graduate School of Natural Science and Technology, Okayama University, Okayama 700-8530, Japan  
E-mail: minami@suri.sys.okayama-u.ac.jp, h-tanimoto@suri.sys.okayama-u.ac.jp, yanou@suri.sys.okayama-u.ac.jp, tikurin7@suri.sys.okayama-u.ac.jp  
(Received March 18, 2013)  
(Revised July 23, 2013)

and force control method with passivity-based approach [16] has been reported, whose approach is characterized by its assumption that the environment the robot is contacting should be deformable like spring. An exponentially stable adaptive controller [17] has been also published based on the same assumption of deformable environment. Contrasting to the above previous researches, our proposed method abstracted below is not based on the deformable assumption but rigid environment whose expression of constraint condition can be represented by algebraic equations, featuring in not utilizing force measurement feedback like [18].

The following equation (1), which has been pointed out by Hemami [19] in the analysis of biped walking robot, denotes also algebraic relation between the input torque  $\tau$  of the robot and exerting force  $F_n$  to the working object, when robot's end-effector being in touch with a surface in 3-D space:

$$F_n = a(\mathbf{x}_1, \mathbf{x}_2) - \mathbf{A}(\mathbf{x}_1)\tau, \quad (1)$$

where,  $\mathbf{x}_1$  and  $\mathbf{x}_2$  are state variables.  $a(\mathbf{x}_1, \mathbf{x}_2)$  and  $\mathbf{A}(\mathbf{x}_1)$  are a scalar function and a vector one defined in following section. A strategy to control force and position proposed in this paper is also based on (1). Contrarily to Peng's Method [7] to use (1) as a force sensor, we use the equation for calculating  $\tau$  to achieve a desired exerting force  $F_{nd}$  [20]–[22].

In this paper, position and force control performances of our new controller [20] are confirmed by grinding experiments, especially on the view point that the force control space and the position control space are divided into orthogonal spaces being complement each other, that is, force space is defined by range space of  $\mathbf{A}$  and the other is the null space of  $\mathbf{A}$ ,  $(\mathbf{I} - \mathbf{A}^+\mathbf{A})$ .

The problem to be solved in our approach is that the mathematical expression of algebraic constraint condition should be included in the controller in order to develop a force/position controller without force sensor. Grinding task requires on-line estimation of changing constraint condition since the grinding is the action to change the constraint condition in nature, which we have presented in previous report [22] evaluated by simulations. The grinding tasks can be generally categorized into two cases. The first case is to be focused on the uniform removal from the initial contour of the workpiece, and the second case is to accurately create a surface based on a designed model like 3D-CAD. The proposed method belongs to the second case, that is, one of the aims of this paper is to develop a force-sensorless shape-grinding system. According to the orientation of the grinding wheel, the following three cases can be considered: (A) the grinding wheel is contacted to the workpiece with a surface and its surface is the circular area of the grinding wheel, (B) the grinding wheel is contacted to the workpiece with a line, whose length is the thickness of the grinding wheel and (C) the grinding wheel is contacted to the workpiece with an edge of the grinding wheel as shown in Fig. 1. Among these cases, this paper deals with the case of (C) only. Other cases, (A) and (B), are not dealt with. The contact edge changes as the robot moves, in the case of (C). It means that the control of the case of (C) is attractive and challenging since the case of (C) — point-contacting other than surface contacting — can be thought to be effective for shape-grinding through direct force controlling strategy proposed in this paper.

This paper has confirmed the feasibility of the proposed method of direct force control. We estimate the object's sur-

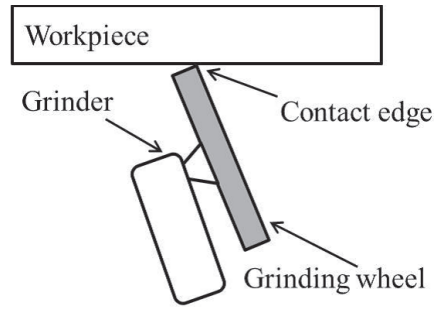


Fig. 1 Relation between workpiece and grinding wheel.

face using the grinder as a touch sensor. In order to give the system the ability to grind any working object into any shape, we focus on how to update the constraint condition in real time, obtaining the result that spline function is best for on-line shape estimation. Based on the above preparation the authors constructed a continuous shape-grinding experiment to evaluate the proposed shape-grinding system, which aims for grinding to desired shape without force sensor.

## 2. Analysis of Grinding Task

Generally speaking, the grinding power is related to the metal removal rate (weight of metal being removed within unit time), which is determined by the depth of cut, the width of cut, the linear velocity of the grinding wheel, the feed rate and so on. There are many empirical formulae available for the determination of grinding power, and the desired force trajectory can then be planned according to the power. The normal grinding force  $F_n$  is exerted in the perpendicular direction of the surface. It is a significant factor that affects ground accuracy and surface roughness of work-piece. The value of it is also related to the grinding power or directly to the tangential grinding force as

$$F_t = K_t F_n, \quad (2)$$

where,  $K_t$  is an empirical coefficient,  $F_t$  is the tangential grinding force. Although friction forces such as viscous friction and Coulomb friction are important factors for the efficiency of grinding task, the behavior of the dynamics of manipulator with grinder's wheel and contacting workpiece and its stability, for simplicity of discussion, this paper summarizes their friction forces to  $F_t$  based on an empirical coefficient  $K_t$  in (2). The axial grinding force  $F_s$  is proportional with the feed rate. In other words,  $F_s$  depends on velocity of grinder contacted on grinding surface. The velocity is mainly determined by position (velocity) feedback controller as shown in Fig. 2. The velocity is not so much faster in this paper because one of the aims of this paper is shape-grinding. Therefore the axial grinding force is much smaller than the tangential grinding force. The details have been written in the book [23].

Equation (2) is based on the situation that position of the grinding cutter is controlled like currently used machining center. But when a robot is used for the grinding task, the exerting force to the object and the position of the grinding cutter should be controlled simultaneously. The exerting force  $F_n$  is generally determined by the constrained situation, and it is not suitable to apply (2) to grinding motion by the robots.

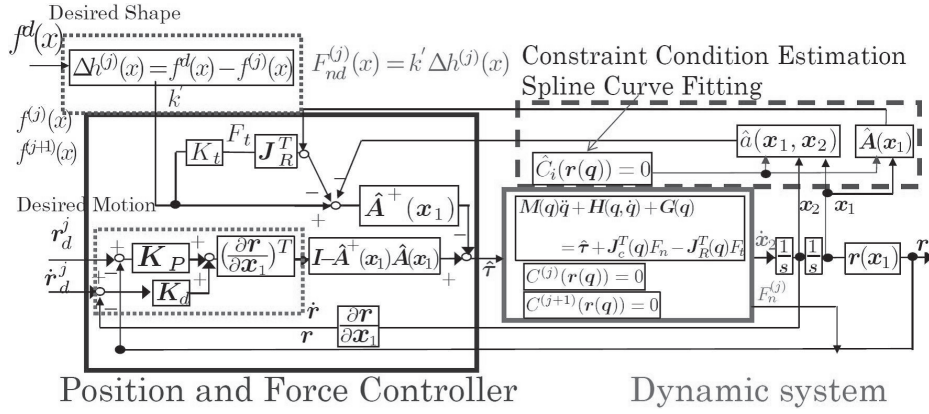


Fig. 2 Shape-grinding position/force control system.

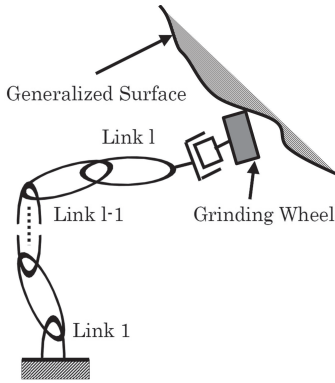


Fig. 3 Grinding robot.

### 3. Modeling

#### 3.1 Constrained Dynamic Systems

Hemami and Wyman have addressed the issue of control of a moving robot according to a constraint condition and examined the problem of the control of the biped locomotion constrained in the frontal plane. Their purpose was to control the position coordinates of the biped locomotion rather than generalized forces of constrained dynamic equation involved the item of generalized forces of constraints. And the constrained force is used as a determining condition to change the dynamic model from constrained motion to free motion of the legs. In this paper, the grinding manipulator shown in Figs. 1 and 3, whose end-point is in contact with the constrained surface, is modeled according (3) with Lagrangian equations of motion in terms of the constraint forces, referring to what Hemami and Arimoto have done:

$$\frac{d}{dt} \left( \frac{\partial L}{\partial \dot{q}} \right) - \left( \frac{\partial L}{\partial q} \right) = \tau + J_c^T(q)F_n - J_r^T(q)F_t, \quad (3)$$

where,  $J_c$  and  $J_r$  satisfy,

$$J_c = \frac{\partial C}{\partial q} \left/ \left\| \frac{\partial C}{\partial r} \right\| \right. = \frac{\partial C}{\partial r} \tilde{J}_r \left/ \left\| \frac{\partial C}{\partial r} \right\| \right.,$$

$$\tilde{J}_r = \frac{\partial r}{\partial q}, \quad J_r^T = \tilde{J}_r^T \dot{r} / \|\dot{r}\|,$$

$r$  is the  $l$  position vector of the hand and can be expressed as a kinematic equation ,

$$r = r(q). \quad (4)$$

$L$  is the Lagrangian function,  $q$  is  $l$  ( $\geq 2$ ) generalized coordinates,  $\tau$  is  $l$  inputs. The discussing robot system does not have

kinematical redundancy.  $C$  is a scalar function of the constraint, and is expressed as an equation of constraints

$$C(r(q)) = 0, \quad (5)$$

$F_n$  is the constrained force associated with  $C$  and  $F_t$  is the tangential disturbance force.

Equation (3) can be derived to be

$$M(q)\ddot{q} + H(q, \dot{q}) + G(q) = \tau + J_c^T(q)F_n - J_r^T(q)F_t, \quad (6)$$

where  $M$  is an  $l \times l$  matrix,  $H$  and  $G$  are  $l$  vectors. The state variable  $x$  is constructed by adjoining  $q$  and  $\dot{q}$ :  $x = (x_1^T, x_2^T)^T = (q^T, \dot{q}^T)^T$ . The state-space equation of the system are

$$\begin{aligned} \dot{x}_1 &= x_2, \\ \dot{x}_2 &= -M^{-1}(H(x_1, x_2) + G(x_1)) \\ &\quad + M^{-1}(\tau + J_c^T(x_1)F_n - J_r^T(x_1)F_t), \end{aligned} \quad (7)$$

or in the compact form

$$\dot{x} = F(x, \tau, F_n, F_t), \quad (8)$$

Using the inverted form of combination from (5) and (8) (this part had been detailedly introduced in [22] by the authors),  $F_n$  can be expressed as

$$F_n = F_n(x, \tau, F_t), \quad (9)$$

or in a more detailed form

$$\begin{aligned} F_n &= \left[ \left( \frac{\partial C}{\partial q} \right) M^{-1} \left( \frac{\partial C}{\partial q} \right)^T \right]^{-1} \left\| \frac{\partial C}{\partial r} \right\| \\ &\quad \left\{ - \left[ \frac{\partial}{\partial q} \left( \frac{\partial C}{\partial q} \right) \right] \dot{q} + \left( \frac{\partial C}{\partial q} \right) M^{-1} (H(q, \dot{q}) + G(q) + J_r^T F_t) \right\} \\ &\quad - \left[ \left( \frac{\partial C}{\partial q} \right) M^{-1} \left( \frac{\partial C}{\partial q} \right)^T \right]^{-1} \left\| \frac{\partial C}{\partial r} \right\| \left\{ \left( \frac{\partial C}{\partial q} \right) M^{-1} \right\} \tau \\ &\triangleq a(x_1, x_2) + A(x_1) J_r^T F_t - A(x_1) \tau, \end{aligned} \quad (10)$$

where,  $a(x_1, x_2)$  is a scalar representing the first term in the expression of  $F_n$ , and  $A(x_1)$  is an  $l$  vector to represent the coefficient vector of  $\tau$  in the same expression. Equations (8) and (9) compose a constrained system that can be controlled, if  $F_n = 0$ , describing the unconstrained motion of the system.

Substituting (10) into (7), the state equation of the system including the constrained force (as  $F_n > 0$ ) can be rewritten as

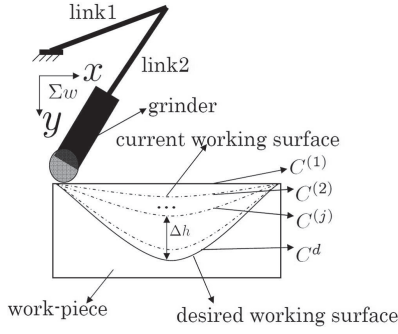


Fig. 4 Model of shape-grinding.

$$\begin{aligned} \dot{\mathbf{x}}_1 &= \mathbf{x}_2, \\ \dot{\mathbf{x}}_2 &= -\mathbf{M}^{-1}[\mathbf{H}(\mathbf{x}_1, \mathbf{x}_2) + \mathbf{G}(\mathbf{x}_1) - \mathbf{J}_c^T(\mathbf{x}_1)\mathbf{a}(\mathbf{x}_1, \mathbf{x}_2)] \\ &\quad + \mathbf{M}^{-1}[(\mathbf{I} - \mathbf{J}_c^T \mathbf{A})\boldsymbol{\tau} + (\mathbf{J}_c^T \mathbf{A} - \mathbf{I})\mathbf{J}_r^T \mathbf{F}_r], \end{aligned} \quad (11)$$

Solutions of these dynamic equations always satisfy the constrained condition (5).

### 3.2 Shape-Grinding

In the past, the authors did the continuous shape grinding simulations [22] to try to extend the grinding ability of our grinding robot [20]. In this paper, the continuous shape grinding experiment which has been done by the proposed force sensorless position/force control method will be introduced.

To make the grinding task to be different from the former flat grinding experiment [20], we want to grind the work-piece into the one with different kinds of shapes, for example, grinding the flat surface into a curved one, just like Fig. 4. In Fig. 4, we can find that the desired working surface is prescribed (it can be decided by the authors), which means the desired constrained condition  $C^d$  is known, so

$$C^d = y - f^d(x) = 0 \quad (12)$$

But the constrained condition  $C^{(j)}$  ( $j = 1, 2, \dots, d-1$ ) changed by the previous grinding which is in the Dynamic System of Fig. 2 is hard to define as an initial condition. Thus we define

$$C^{(j)} = y - f^{(j)}(x) = 0 \quad (13)$$

where,  $y$  is the  $y$  position of manipulator's end-effector in the coordinates  $\Sigma_w$  depicted in Fig. 4 and we assume  $C^{(1)}$  is known, that is to say,  $f^{(1)}(x)$  is initially defined.  $f^{(j)}(x)$  is the working surface remained by  $i$ -th grinding. And  $f^{(j)}(x)$  is a function passing through all points,  $(x_1, f^{(j)}(x_1)), (x_2, f^{(j)}(x_2)), \dots, (x_p, f^{(j)}(x_p))$ , these observed points representing the  $(j)$ -th constraint condition obtained from the grinding tip position since the authors proposed previously the grinding tip used for the touching sensor of ground new surface. Here we assume  $f^{(j)}(x)$  could be represented by a polynomial of  $(p-1)$ -th order of  $x$ . Given the above  $p$  points, we can easily decide the parameters of polynomial function  $y = f^{(j)}(x)$ . If the current constrained condition can be got successfully, which means the current working surface  $f^{(j)}(x)$  can be detected correctly, the distance from the current working surface to the desired working surface which is expressed as  $\Delta h^{(j)}$  shown in Fig. 4 can be obtained easily.

$$\Delta h^{(j)}(x_i) = f^d(x) \Big|_{x=x_i} - f^{(j)}(x) \Big|_{x=x_i} \quad (14)$$

In this case, we can obviously find that the desired constrained force should not be a constant. It should be changed while  $\Delta h^{(j)}$

changes. Thus we redefine the desired constrained force  $F_{nd}^{(j)}$  as a function of  $\Delta h^{(j)}$ , shown as follows:

$$F_{nd}^{(j)}(x_i) = k' \Delta h^{(j)}(x_i) \quad (15)$$

where  $k'$  [N/m] is a constant, and  $k' = 1000$  N/m heuristically in our experiment.

## 4. Force and Position Controller

### 4.1 Controller Using Estimated Constraint Condition

Reviewing the dynamic equation (3) and constraint condition (5), it can be found that as  $l > 1$ , the number of input generalized forces is more than that of the constrained forces. From this point and (10) we can claim that there is some redundancy of constrained force between the input torque  $\boldsymbol{\tau}$ , and the constrained force  $F_n$ . This condition is much similar to the kinematical redundancy of redundant manipulator. Based on the above argument and assuming that, the parameters of the (10) are known and its state variables were able to be measured, and  $\mathbf{a}(\mathbf{x}_1, \mathbf{x}_2)$  and  $\mathbf{A}(\mathbf{x}_1)$  were able to be calculated correctly, which means that the constraint condition  $C = 0$  is prescribed. As a result, a control law is derived and can be expressed as

$$\begin{aligned} \boldsymbol{\tau} &= -\mathbf{A}^+(\mathbf{x}_1) \left\{ F_{nd} - \mathbf{a}(\mathbf{x}_1, \mathbf{x}_2) - \mathbf{A}(\mathbf{x}_1) \mathbf{J}_R^T \mathbf{F}_r \right\} \\ &\quad + (\mathbf{I} - \mathbf{A}^+(\mathbf{x}_1) \mathbf{A}(\mathbf{x}_1)) \mathbf{k}, \end{aligned} \quad (16)$$

where  $\mathbf{I}$  is a  $l \times l$  identity matrix,  $F_{nd}$  is the desired constrained forces,  $\mathbf{A}(\mathbf{x}_1)$  is defined in (10) and  $\mathbf{A}^+(\mathbf{x}_1)$  is the pseudoinverse matrix of it,  $\mathbf{a}(\mathbf{x}_1, \mathbf{x}_2)$  is also defined in (10) and  $\mathbf{k}$  is an arbitrary vector which is defined as

$$\mathbf{k} = \tilde{\mathbf{J}}_r^T(\mathbf{q}) \left\{ \mathbf{K}_p(\mathbf{r}_d - \mathbf{r}) + \mathbf{K}_d(\dot{\mathbf{r}}_d - \dot{\mathbf{r}}) \right\}, \quad (17)$$

where  $\mathbf{K}_p$  and  $\mathbf{K}_d$  are gain matrices for position and the velocity control by the redundant degree of freedom of  $\mathbf{A}(\mathbf{x}_1)$ ,  $\mathbf{r}_d(\mathbf{q})$  is the desired position vector of the end-effector along the constrained surface and  $\mathbf{r}(\mathbf{q})$  is the real position vector of it. Equation (17) describes the 2-link rigid manipulator's arm compliance. We have to set  $\mathbf{K}_p$  and  $\mathbf{K}_d$  with a reasonable value, otherwise high-frequency response of position error will appear. The controller presented by (16) and (17) assumes that the constraint condition  $C = 0$  be known precisely even though the grinding operation is a task to change the constraint condition. This looks like to be a contradiction, and hence we need to observe time-varying constraint conditions in real time, that is, the actual shape by using grinding tip as a touch sensor. The time-varying condition is estimated as an approximate constrained function by position of the manipulator hand, which is based on the estimated constrained surface location. The estimated condition is denoted by  $\hat{C} = 0$  (in this paper, “ $\hat{\phantom{x}}$ ” means the situation of unknown constraint condition). Hence,  $\mathbf{a}(\mathbf{x}_1, \mathbf{x}_2)$  and  $\mathbf{A}(\mathbf{x}_1)$  including  $\partial \hat{C} / \partial \mathbf{q}$  and  $\partial / \partial \mathbf{q} (\partial \hat{C} / \partial \mathbf{q})$  are changed to  $\hat{\mathbf{a}}(\mathbf{x}_1, \mathbf{x}_2)$  and  $\hat{\mathbf{A}}(\mathbf{x}_1)$  as shown in (19) and (20). They were used in the later experiments of the unknown constrained condition. As a result, a controller based on the estimated constrained condition is given as

$$\begin{aligned} \hat{\boldsymbol{\tau}} &= -\hat{\mathbf{A}}^+(\mathbf{x}_1) \left\{ F_{nd} - \hat{\mathbf{a}}(\mathbf{x}_1, \mathbf{x}_2) - \hat{\mathbf{A}}(\mathbf{x}_1) \mathbf{J}_R^T \mathbf{F}_r \right\} \\ &\quad + (\mathbf{I} - \hat{\mathbf{A}}^+(\mathbf{x}_1) \hat{\mathbf{A}}(\mathbf{x}_1)) \mathbf{k}, \end{aligned} \quad (18)$$

$$m_c^{-1} \left\| \frac{\partial \hat{C}}{\partial \mathbf{r}} \right\| \left\{ - \left[ \frac{\partial}{\partial \mathbf{q}} \left( \frac{\partial \hat{C}}{\partial \mathbf{q}} \right) \dot{\mathbf{q}} \right] \dot{\mathbf{q}} + \left( \frac{\partial \hat{C}}{\partial \mathbf{q}} \right) \mathbf{M}^{-1} (\mathbf{h} + \mathbf{g}) \right\} \triangleq \hat{\mathbf{a}}(\mathbf{x}_1, \mathbf{x}_2) \quad (19)$$

$$m_c^{-1} \left\| \frac{\partial \hat{C}}{\partial \mathbf{r}} \right\| \left\{ \left( \frac{\partial \hat{C}}{\partial \mathbf{q}} \right) \mathbf{M}^{-1} \right\} \triangleq \hat{\mathbf{A}}(\mathbf{x}_1) \quad (20)$$

Figure 2 illustrates a control system constructed according to the above control law that consists of a position feedback control loop and a force feedforward control. Although force feedback control through force sensor enables us to make the controlled grinding force follow the desired one, which has been well discussed by other researchers, the authors believe that force-sensorless system is desirable in the shape-grinding situation with many of strong contacts, because force sensor is delicate and costly. Therefore, as we have addressed the merits of force-sensorless grinding controller in introduction, the aim of our approach is to construct force-sensorless shape-grinding system. The proposed controller is calculated by manipulator's kinematics and constructed by the position feedback control and the force feedforward control, under the assumption that the manipulator's kinematics is precisely given.

It can be found from (10) and (18) that the constrained force always equals to the desired one explicitly if the estimated constraint condition equals to the real one, i.e.,  $C = \hat{C}$  and  $F_t = 0$ . This is based on the fact that force transmission is an instant process. In the next section, we will introduce an estimation method which is used to get  $\hat{C}$  in current time.

#### 4.2 On-Line Estimation Method of Constraint

Now shape-grinding method is given to be solved in this research. But how to estimate the unknown constraint surface is the nodus and key point. Here, an unknown constrained condition is assumed as following,

Assumptions:

1. The end point position of the manipulator during performing the grinding task can be surely measured and updated.
2. The grinding task is defined in  $x - y$  plane.
3. When beginning to work, the initial condition of the end-effector is known and it has touched the work object.
4. The chipped and changed constraint condition can be approximated by connections of minute sections.

Some fundamental relations between position value and time value are described here.

$$x_{i-1} = x(t_{i-1}) = x(t_0 + (i-1)\Delta t), \quad (21)$$

$$x_i = x(t_i) = x(t_0 + i\Delta t), \quad (22)$$

$$x_{i+1} = x(t_{i+1}) = x(t_0 + (i+1)\Delta t). \quad (23)$$

Before on-line estimation method is introduced, let's take a look at the situation of known flat constraint surface. For example, just like the grinding surface shown in Fig. 5, the expression of this surface is straight linear equation

$$f^j(x_i) = y_i \quad (i = 0, 1, 2, 3 \dots n), \quad (24)$$

and point  $(x_i, y_i)$  is the current position of grinding robot's end-effector. As a result, points before  $(x_i, y_i)$  have been already ground by grinder when  $t \leq t_0 + i\Delta t$ . In the next moment, when time  $t_{i+1} = t_0 + (i+1)\Delta t$ , constraint condition

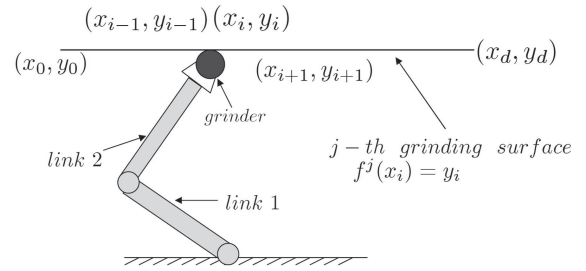


Fig. 5 Situation of known constraint surface model.

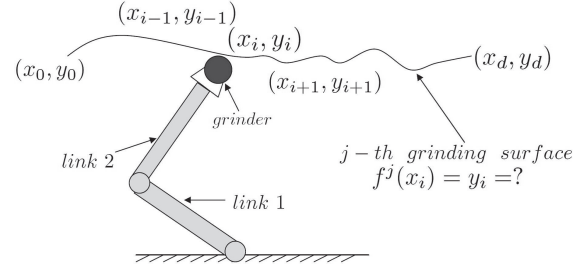


Fig. 6 On-line estimation model.

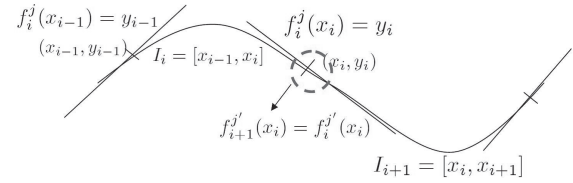


Fig. 7 Fitting by quadratic spline curve.

$$C_{i+1}^j = y - f^j(x_i) = 0 \quad (25)$$

can be used for calculation of deriving torque  $\tau$ . And also, grinder will move to next point  $(x_{i+1}, y_{i+1})$  with no hesitation driven by the input torque  $\tau$ . The term, "with no hesitation", means that no this known surface, grinder has nowhere to go but point  $(x_{i+1}, y_{i+1})$ , since this whole grinding surface  $f^j(x_i) = y_i$  ( $i = 0, 1, 2, 3 \dots n$ ) is determined obviously. However, we all know that the grinding surface on work-piece after ground will turn into some kind of irregular shape that no mathematic equation can express. What should we do to obtain the future constraint condition  $C_{i+1}^j$  if the grinding surface is unknown? Like the situation shown in Fig. 6, the grinding surface is not a simple straight line or some curve line which can be defined and expressed by some certain curve equation, after current time  $t_i = t_0 + i\Delta t$ , where should the grinder go? Grinding robot has no idea since input torque  $\tau$  cannot be derived without constraint condition  $C_{i+1}^j$ . To solve this problem, we consider that some kind of on-line estimation function should be utilized to imitate the unknown grinding surface, in order to obtain an unknown constraint condition  $\hat{C}_{i+1}^j$ , which can be used to calculate the input torque  $\hat{\tau}$ .

Therefore, now let's take a look at Fig. 6, in current time  $t_i = t_0 + i\Delta t$ , end-effector of grinding robot is at position  $(x_i, y_i)$ , so far, point  $(x_{i-1}, y_{i-1})$  and point  $(x_i, y_i)$  have become known because they were just ground by the grinder in the moment  $t_{i-1} = t_0 + (i-1)\Delta t$  and  $t_i = t_0 + (i)\Delta t$  and the information of point  $(x_{i-1}, y_{i-1})$  and  $(x_i, y_i)$  can be derived through the position of robot's end-effector. Now building an estimation function going through these two points, for example, a quadratic spline function

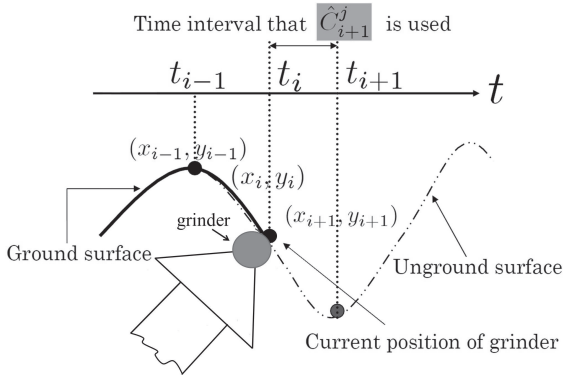


Fig. 8 Expansion of interval between point  $(x_{i-1}, y_{i-1})$  and point  $(x_{i+1}, y_{i+1})$  on the on-line estimation model.

$$\begin{aligned} f_i^j(x_i) &= f_{spline}(x_i) = y_i \\ &= \alpha_i(x - x_{i-1})^2 + \beta_i(x - x_{i-1}) + \gamma_i \\ x &\in [x_{i-1}, x_i] \quad (i = 0, 1, 2, 3 \dots n), \end{aligned} \quad (26)$$

we can figure out the coefficients  $\alpha_i$ ,  $\beta_i$  and  $\gamma_i$  uniquely according to the information of points  $(x_{i-1}, y_{i-1})$ ,  $(x_i, y_i)$  and derivation at point  $(x_i, y_i)$  as follows.

Let  $f_i^j(x_i)$  satisfy the following conditions shown in Fig. 7.

(A) Go through two ends of the interval

$$y_{i-1} = f_i^j(x_{i-1}) \quad (27)$$

$$y_i = f_i^j(x_i). \quad (28)$$

(B) First derivatives of the spline polynomials are equal at the end-point of adjoined function.

$$f_{i+1}^j(x_i) = f_i^j(x_i). \quad (29)$$

From the relations among (26), (27), (28) and (29), we can obtain:

$$\gamma_i = y_{i-1}, \quad (i = 1, 2, \dots, n) \quad (30)$$

$$\beta_{i+1} = 2u_i - \beta_i, \quad (i = 1, 2, \dots, n-1) \quad (31)$$

$$\alpha_i = \frac{\beta_{i+1} - \beta_i}{2h_i}, \quad (i = 1, 2, \dots, n-1). \quad (32)$$

Where,  $h_i = x_i - x_{i-1}$ ,  $u_i = \frac{y_i - y_{i-1}}{h_i}$ . The above-mentioned result can update the constrained conditional expression  $\hat{C}_{i+1}^j$  step by step.

Making an expansion of the interval between point  $(x_{i-1}, y_{i-1})$  and point  $(x_{i+1}, y_{i+1})$  on the grinding surface which is shown in Fig. 8, we can see the first half of grinding surface before the current position - point  $(x_i, y_i)$  is shown by black line, which means this part has been already ground, and second half after point  $(x_i, y_i)$  is shown by break point line, which means this part has not been ground yet. Now let's pay our attention on the interval between point  $(x_i, y_i)$  and point  $(x_{i+1}, y_{i+1})$ , which means this part has been estimated by quadratic spline function. With the estimation function the next point  $(x_{i+1}, y_{i+1})$  can easily be found to be known, and then this point can be the position where grinder should go in the next moment when  $t_{i+1} = t_0 + (i+1)\Delta t$ . At the same time, this imitative function can be used as the on-line estimation function to obtain the unknown constraint condition

$$\begin{aligned} \hat{C}_{i+1}^j &= y - f_i^j(x) \\ &= y - [\alpha_i(x - x_{i-1})^2 + \beta_i(x - x_{i-1}) + \gamma_i] = 0, \\ &(x_i \leq x \leq x_{i+1}) \end{aligned} \quad (33)$$

Table 1 Parameters of grinding robot.

	link 1	link 2
mass of link (kg)	$m_1 = 12.28$	$m_2 = 7.64$
length of link (m)	$l_1 = 0.3$	$l_2 = 0.5$
gravity center of link (m)	$a_1 = 0.24$	$a_2 = 0.25$
general coordinates (rad)	$q_1$	$q_2$
input torque (N)	$\hat{\tau}_1$	$\hat{\tau}_2$

during the period when grinder goes from point  $(x_i, y_i)$  to point  $(x_{i+1}, y_{i+1})$ , which means in this unknown interval on the grinding surface, the future unground part  $(x_i, y_i)$  to  $(x_{i+1}, y_{i+1})$  can be ground by this on-line estimation method based on the information obtained from already ground part  $(x_{i-1}, y_{i-1})$  to  $(x_i, y_i)$ . Thus, in the situation of unknown constraint surface, using this on-line estimation method point to point, the problem for grinding robot that it doesn't know where it should go in future time can be solved theoretically.

## 5. Experiment

### 5.1 Experiment Purpose and Devices

In this section, we will introduce a curve surface shape-grinding experiment on an iron work-piece with this proposed position/force control method. During this experiment, constraint condition  $\hat{C}_{i+1}^j$  which has been explained before is always changing because of the changing constraint working surface. Based on the previous simulation result [22], we choose quadratic spline function to estimate the changing constraint surface and build the constraint condition  $\hat{C}_{i+1}^j$ . Figure 4 shows the experiment's grinding task. In Fig. 4, we can find that the desired surface is known(it can be determined by us, here we use (34) as this desired surface)

$$\begin{aligned} f^d(x_i) &= \left[ 0.5173 + 0.015 \cos(5\pi x_i + \frac{\pi}{2}) \right] \text{m} \\ &(0.0 \leq x_i \leq 0.2 \text{ m}) \end{aligned} \quad (34)$$

and also the initial flat surface is known as (35)

$$f^1(x_i) = 0.5173 \text{ m} \quad (0.0 \leq x_i \leq 0.2 \text{ m}) \quad (35)$$

Here we notice that although the initial constraint surface  $f^1(x_i)$  and desired constraint surface  $f^d(x_i)$  are known already, those functions  $f^j(x_i)$  who can express the constraint working surfaces between  $f^1(x_i)$  and  $f^d(x_i)$  are unknown. Therefore, we utilize the quadratic spline function to estimate them.

$$f^j(x_i) = f_{spline}(x_i) \quad (0.0 \leq x_i \leq 0.2 \text{ m}) \quad (36)$$

The initial constraint surface to be ground is defined as  $(x, y) = (0.0, 0.5173) - (0.2, 0.5173)$  m in time 5.0 s, and the desired velocity along the surface is 0.04 m/s. The desired force,  $F_{nd}$ , is set as

$$F_{nd}^j(x_i) = k' \Delta h^j(x_i) \quad (k' = 1000 \text{ N/m}) \quad (37)$$

$\Delta h(x_i)$  indicates the distance between the current surface and desired surface, shown in Fig. 4.

$$\Delta h^j(x_i) = f^d(x_i) - f^j(x_i) = f^d(x_i) - f_{spline}(x_i) \quad (38)$$

Grinding robot's parameters are listed in Table 1, and there are two motors (produced by Yaskawa Ltd.) mounted on those two links used in torque control mode whose output torque can be designated by the input voltage to the amplifier to each motor, where motor of AC(400 W, 200 V) drives link 1, motor of

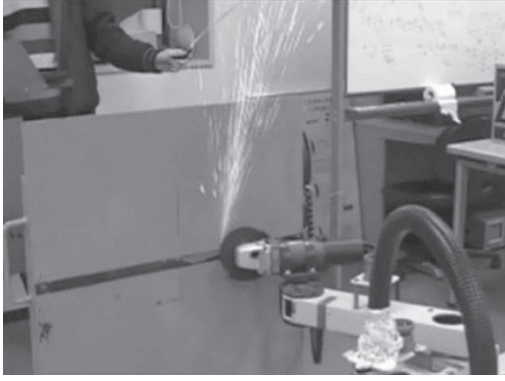


Fig. 9 Performance of shape-grinding experiment.

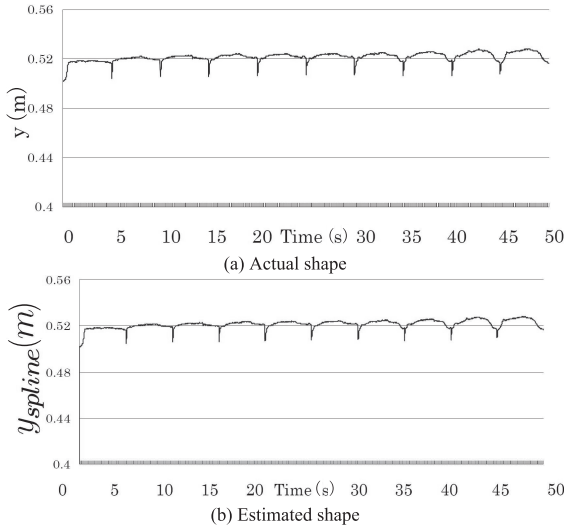


Fig. 10 Comparison of actual and estimated shape during 10 times' experiment.

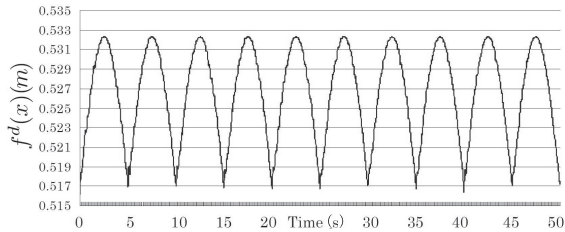
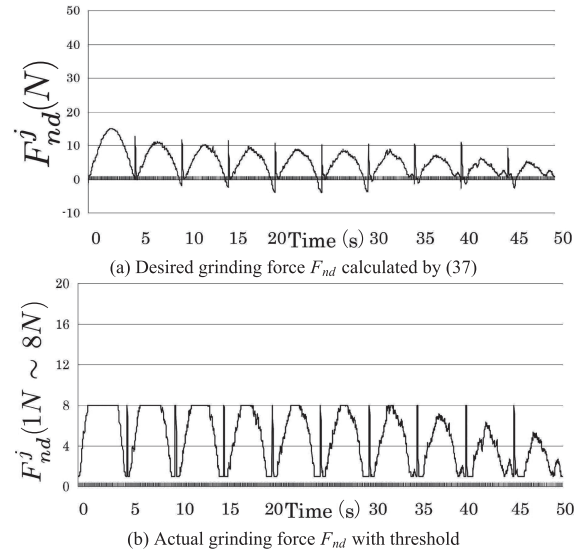
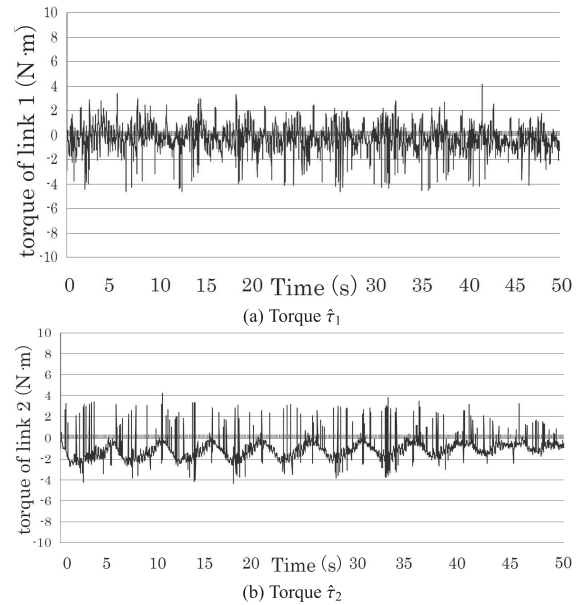


Fig. 11 Desired shape of grinding experiment.

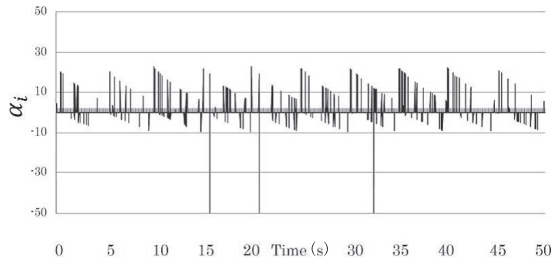
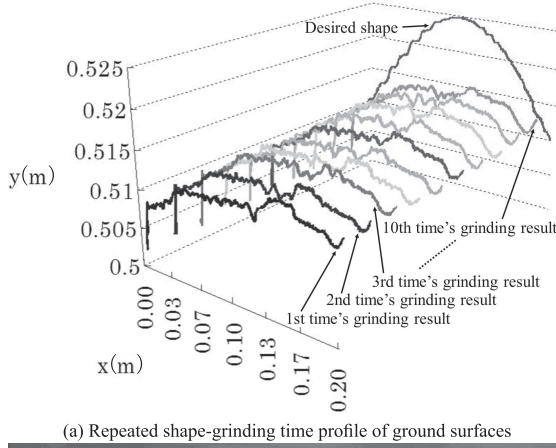
AC (200 W, 200 V) drives link 2. Link 1's Torque/Voltage is 0.42 Nm/V, link 2's Torque/Voltage is 0.21 Nm/V. JIS material symbol of the iron work-piece to be ground is SS400. The material of grinding wheel is synthetic resin, and its specification is 100 mm (outer diameter)  $\times$  3 mm (thickness) and F36 (grain size).

## 5.2 Experiment Results 1

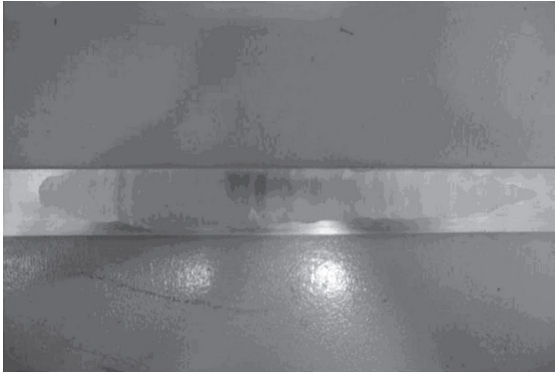
This section shows the 10 times' shape-grinding experiment result. It takes 5 s for each time, and hence, in total there are 50 s had been used to do this experiment. Figure 9 shows the performance of this grinding robot during 10 times' shape grinding experiment. Figure 10 (a) shows the 10 times' working surfaces ground by robot's grinder, which is mounted on the tip of grinding robot's hand, and meanwhile Fig. 10 (b) has recorded the surfaces' functions which are estimated by quadratic spline function. Comparing these two figures, we

Fig. 12 Desired constraint force  $F_{nd}$  decided by  $\Delta h$  in 10 times' experiment.Fig. 13 Change of torque  $\hat{\tau}_{1,2}$  during 10 times' experiment.

can tell that the estimated trajectory has almost the same value of the real ground surfaces. Desired shape of this experiment has been recorded and shown in Fig. 11. Here we set the desired shape as a curve with a deepest position 150 mm, and the work-piece used in this shape-grinding experiment is an iron board, which is very hard to grind, and hence if we want to grind the whole curve shape, experiment should be done by almost 300 times. But to verify the effectiveness of this force-sensorless position/force control method, 10 times' continuous shape-grinding experiment will do if we can obtain an obvious small curve shape after grinding work. Therefore, although this very deep desired curve shape has been set, it is just used as a generator of desired grinding force  $F_{nd}$  through (37). The desired grinding force  $F_{nd}$  calculated by (37) is shown by Fig. 12 (a). From this figure, we can see that the desired grinding force's value is bigger than 10 N sometimes, and smaller than 0 N at the beginning point, and hence to make sure that stable touch between grinder and work-piece can be obtained

Fig. 14 Change of spline function's coefficient  $\alpha_i$  in Eq.(32).

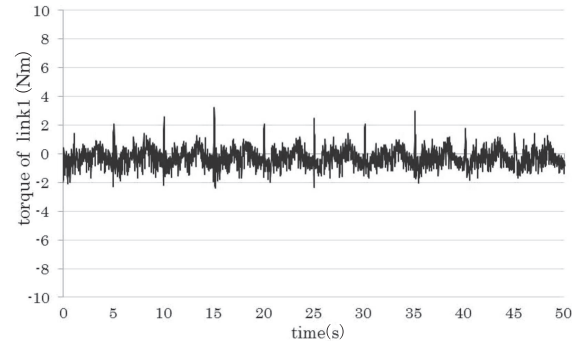
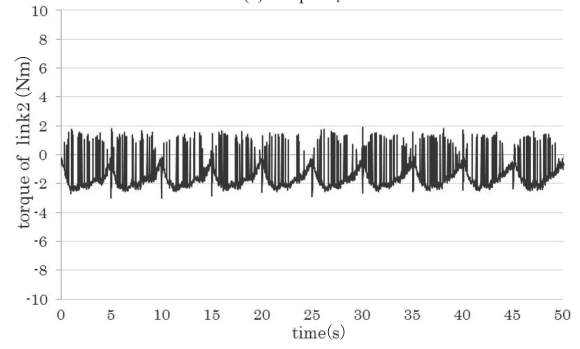
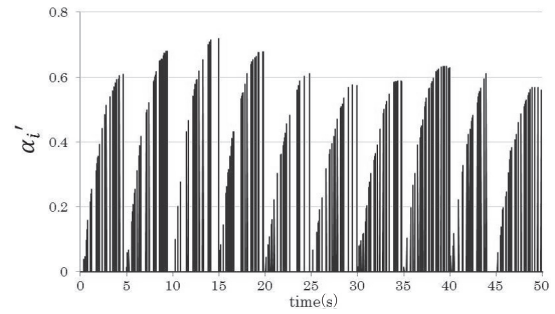
(a) Repeated shape-grinding time profile of ground surfaces



(b) Photograph of ground iron specimen

Fig. 15 Real ground and desired surface, and its appearance.

in order to do this grinding experiment safely, in the controller system we set a threshold to select those safe and useful value to be utilized, which is shown by Fig. 12 (b). The input torques  $\hat{\tau}_{1,2}$  calculated with the unknown constraint condition  $\hat{C}$  are shown in Fig. 13. Since the unknown constraint condition  $\hat{C}$  is built by quadratic spline estimation method, the vibration of quadratic spline function's coefficient  $\alpha_i$  (shown in Fig. 14) is affecting the input torques  $\hat{\tau}_{1,2}$  during the whole experiment time. Figure 15 (a) shows 10 times' continuous shape-grinding experiment result. From this side, each line means the real ground surfaces from 1st to 10th shape-grinding experiment and desired surface. After 10 times grinding, the iron board can be ground as Fig. 15 (b), and also a small curve shape has been ground out although the iron board is very hard to grind. The difference of the experimental condition between Figs. 10 and 15 is material of work-piece to be ground. Although the specimen used in Fig. 10 has been discarded unfortunately, the material used in Fig. 15 is SS400 in the JIS material symbol. In this experiment, each x-y position in Fig. 15 (a) is obtained from the manipulator's kinematics, not the measurement result of x-y positions by stylus instrument, because one of the aims

(a) Torque  $\hat{\tau}_1$ (b) Torque  $\hat{\tau}_2$ Fig. 16 Change of torque  $\hat{\tau}_{1,2}$  during 10 times' experiment.Fig. 17 Change of filtered spline function's coefficient  $\alpha'_i$ .

of this paper is the verification of shape-grinding result on a prerequisite of the manipulator being used as grinder and also measuring touching sensor. This point is our stressing realistic merit of our system.

Through this 10 times' continuous shape-grinding experiment result, the effectiveness and feasibility of force-sensorless position/force control method can be verified.

### 5.3 Experiment Results 2

The previous subsection shows real ground surfaces can reach the desired surface by grinding a small curve shape repeatedly. But there is a problem that the vibration of spline function's coefficient  $\alpha_i$  shown in Fig. 14 affects the input torques  $\hat{\tau}_{1,2}$  shown in Fig. 13. That is, the problem also causes a vibration of constraint grinding force and rough grinding surface. Therefore this subsection newly introduces a low pass filter to calculate of spline function's coefficient  $\alpha_i$  and give the continuous shape-grinding experimental result aiming to diminish its vibration. The low pass filter in this experiment is given as follows,

$$\alpha'_i = \frac{\Delta t}{T + \Delta t} \alpha_i + \frac{T}{T + \Delta t} \alpha'_{i-1} \quad (39)$$

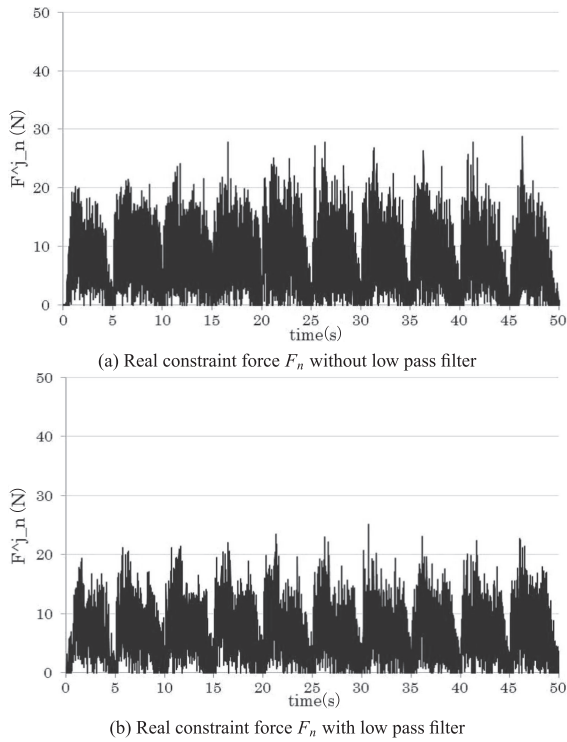


Fig. 18 Real constraint force  $F_n$  measured by force sensor.

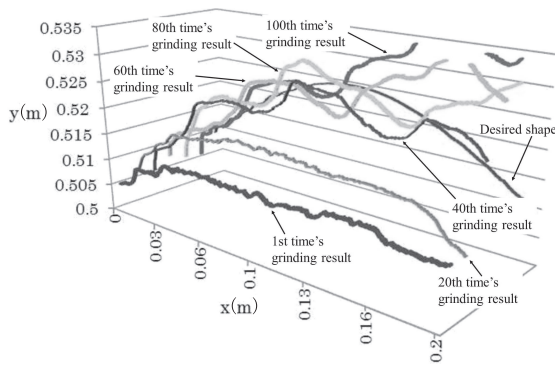


Fig. 19 Real ground surfaces and desired surface.

Where  $T = 5$  and sampling rate  $\Delta t$  is 0.0007 s. The experimental result is shown in Figs. 16–18. And it is noticed that each figure includes 10 times' continuous experiment as described in the previous subsection. Figure 16 shows the input torques  $\hat{\tau}_{1,2}$  when the filter (39) is introduced to the grinding robot system. Comparing to Fig. 13, it can find that the vibration of torque is diminished. And Fig. 17 shows the filtered spline function's coefficient  $\alpha'_i$ . It can also find that the new method in this subsection is superior to Fig. 14 in point of lowering of vibration, and it is noticed that a very small value of  $\alpha_i$  (less than  $-50$ ) is dealt with an exception value and is truncated at  $-20$ . Figure 18 shows the real constraint grinding force measured by a force sensor, and it is noticed that information from this sensor is not applied to control grinding robot in this paper. Figure 18 (a) is the result that did not use the low pass filter (39) and Fig. 18 (b) is the result that used it. From these figures, it is found that the proposed method can lower the vibration of the real constraint grinding force. Therefore the effectiveness of this method can be verified and it is expected that the proposed method achieves a smoother grinding surface than conventional method shown in the previous subsection. In order to realize continuous shape-

grinding system to the desired surface, 100 times' continuous shape-grinding experiment was newly carried out. Then initial position of robot's grinder, when the number of experiments is over about 30 times, was deviating from an original initial position little by little. As a result, the working position of the grinder was rising from and contacting to the real ground surfaces. And the working position of it simply rose from the real ground surfaces after about 50 times' continuous shape-grinding experiment. Figure 19 shows the working position of robot's grinder for 100 times' continuous shape-grinding experiment. In Fig. 19, each line from this side means the real ground surfaces for 1st and 20th shape-grinding experiment, the working position of the grinder for 40th, 60th, 80th and 100th shape-grinding experiment, and desired surface. From Fig. 19, 100 times' continuous shape-grinding experiment in this paper did not go well after about 40th shape-grinding experiment.

## 6. Conclusions

The constraint dynamic equation of manipulator is expressed as a model based function of the manipulator's state and inputs. The manipulator's hand tip is used as a position sensor, to supply those necessary information for this proposed force and position control methodology. The quadratic spline function is chosen to estimate the unknown constraint surface in shape-grinding experiment [22]. 10 times' shape-grinding experiment has been done based on the proposed force and position control law without force or torque sensor. Moreover, in order to lower the vibration of constraint grinding force and make a grinding surface smoother, low pass filter is newly introduced to the grinding robot's system. With comparison to conventional system, the effectiveness of the proposed method is verified. Although 100 times' continuous shape-grinding experiments were also carried out in order to realize a continuous shape-grinding system for the desired surface, as the future works, the problem, that the initial position of robot's grinder deviates from an original initial position little by little, must be solved. In the experiments, we obtained each  $x$ - $y$  position in Figs. 15 and 19 from the manipulator's kinematics, as substitute for the measurements of  $x$ - $y$  positions by a stylus instrument. The experiments required the manipulator used as a grinder and also required measuring touching sensors. This point diminishes the realistic merits of our system. Moreover, because this paper is a fundamental research on grinding robot, the efficiency, the surface quality and the design complexity of the robot according to the demands from actual industrial fields have not been discussed. This point is also one of the future works. For a new challenge, this paper tried to reduce the vibration of input torques by low-pass filter in order to smooth grinding surface and could reduce the magnitude dispersion. But there are more spikes for torque of link 2 in Fig. 16, compared with Fig. 13. Because the controlled torques are calculated from the filtered spline function's coefficient  $\alpha'_i$  shown in Fig. 17, the improvement of low-pass filter should be discussed with the order of spline function. And the authors believe that this force-sensorless position/force control method can be utilized in many robotic control fields.

## References

- [1] M.H. Raibert and J.J. Craig: Hybrid position/force control of manipulators, *Trans. of the ASME, J. of Dynamic Systems*,

- Measurement and Control*, Vol.102, pp.126–133, 1981.
- [2] S. Arimoto: *Mechanics and Control of Robot*, Asakura Publishing, 1990 (in Japanese).
- [3] T. Yoshikawa: Dynamic hybrid position/force control of robot manipulators: Description of hand constraints and calculation of joint driving force, *IEEE J. on Robotics and Automation*, Vol.RA-3, No.5, pp.386–392, 1987.
- [4] L. Whitcomb, S. Arimoto, T. Naniwa, and F. Osaki: Experiments in adaptive model-based force control, *IEEE Control Systems Society*, Vol.16, No.1, pp.49–57, 1996.
- [5] S. Arimoto: Joint-space orthogonalization and passivity for physical interpretations of dextrous robot motions under geometric constraints, *Int. J. of Robust and Nonlinear Control*, Vol.5, pp.269–284, 1995.
- [6] D.Wang and N.H. McClamroch: Position and force control for constrained manipulator motion: Lyapunov's direct approach, *IEEE Trans. Robotics and Automation*, Vol.9, pp.308–313, 1993.
- [7] Z.X. Peng and N. Adachi: Position and force control of manipulators without using force sensors, *Trans. of JSME(C)*, Vol.57, No.537, pp.1625–1630, 1991 (in Japanese).
- [8] J. Roy and L.L. Whitcomb: Adaptive force control of position/velocity controlled robots: Theory and experiment, *IEEE Transactions on Robotics and Automation*, Vol.18, No.2, April, 2002.
- [9] S. Arimoto: *Control Theory of Non-Linear Mechanical Systems*, Oxford University Press, 1996.
- [10] B. Siciliano and L. Villani: *Robot Force Control*, Kluwer Academic Publishers, 1999.
- [11] C. Natale: *Interaction Control of Robot Manipulators*, Springer Tracts in Advanced Robotics, 2003.
- [12] N. Hogan: Impedance control: An approach to manipulation: Part 1: Theory, *J. Dynamic Syst., Measurement Contr.*, Vol.107, pp.1–7, 1985.
- [13] T. Mikolajczyk: Robot application to surface finish machining, *Journal of Polish CIMAC*, Vol.5, No.3, 2010.
- [14] P. Hamelin, P. Bigras, J. Beaudry, P. Richard, and M. Blain: Discrete-time state feedback with velocity estimation using a dual observer: Application to an underwater direct-drive grinding robot, *IEEE/ASME Transactions on Mechatronics*, Vol. 17, No. 1, pp.187–191, 2012.
- [15] Y. Song, W. Liang, and Y. Yang: A method for grinding removal control of a robot belt grinding system, *Journal of Intelligent Manufacturing*, Vol.23, No. 5, pp.1903–1913, 2012.
- [16] B. Siciliano and L. Villani: A passivity-based approach to force regulation and motion control of robot manipulators, *Automatica*, Vol.32, No.3, pp.443–447, 1996.
- [17] L. Villani, C.C. de Wit, and B. Brogliato: An exponentially stable adaptive control for force and position tracking of robot manipulators, *IEEE Trans. Automat. Contr.*, Vol.44, pp.778–802, 1999.
- [18] J. De Schutter and H. Van Brussel: Compliant robot motion 2: A control approach based on external control loops, *Int. J. Robot. Res.*, Vol.7, No.4, pp.18–33, 1988.
- [19] H. Hemami and B.F. Wyman: Modeling and control of constrained dynamic systems with application to biped locomotion in the frontal plane, *IEEE Trans. on Automatic Control*, Vol.AC-24, No.4, pp.526–535, 1979.
- [20] T. Ikeda and M. Minami: Position/force control of a manipulator by using an algebraic relation and evaluations by experiments, *Proceeding of the 2003 IEEE/ASME Int. Conf. on Advanced Intelligent Mechatronics (AIM2003)*, pp.503–508, 2003.
- [21] T. Ikeda and M. Minami: Research of grinding robot without force sensor by using algebraic equation, *Transactions of the Japan Society of Mechanical Engineers (C)*, Vol.71, No.702, pp.270–277, 2005 (in Japanese).

- [22] M. Minami and W. Xu: Shape-grinding by direct position/force control with on-line constraint estimation, *Proceedings of the 2008 IEEE/RSJ International Conference on Intelligent Robots and Systems*, pp.943–948, 2008.
- [23] S. Kawamura: *Grinding and Abrasive Machining*, Kyoritsu Publishing, 1984 (in Japanese).

---

#### Mamoru MINAMI (Member)



He received B.S. and M.S. degrees in aeronautical engineering from the University of Osaka Prefecture in 1978 and 1980, respectively, and Ph.D. degree in Faculty of Engineering from the Kanazawa University in 1992. Since 1994 he has been an Associate Professor of Mechanical Engineering at University of Fukui, then he moved to newly established department of Human and Artificial Intelligence Systems in the same university in 1999. He has been a professor there from 2002 and moved to Graduate School of Natural Science and Technology in Okayama University at April in 2010. His current research interests are in the field of robotics and automation in dynamics, kinematics and control of robots including mobile manipulators, and intelligent motion control. And to research intelligent robot, he has been engaged in machine vision for real-time adaptive operation. He is a member of the Japan Society of Mechanical Engineers, the Robotics Society of Japan, and IEEE.

#### Hiro TANIMOTO



He received his B.S. degree from Okayama University, Japan, in 2011. He is currently a master's course student at Okayama University. His research interests include force/position control and shape-grinding experiment.

#### Akira YANOU (Member)



He received his Ph.D. in Engineering from Okayama University, Japan in 2001. He worked with School of Engineering, Kinki University from 2002 to 2008. In 2009, he joined the Graduate School of Natural Science and Technology, Okayama University, as an Assistant Professor. His research interests include adaptive learning, control and estimation.

#### Masaki TAKEBAYASHI

He received his B.S. and M.S. degrees from Okayama University, Japan, in 2010 and 2012, respectively. His research interests include force/position control and shape-grinding experiment.

---